Molecular Phylogenetics and Evolution 130 (2019) 81–91

Contents lists available at ScienceDirect

Molecular Phylogenetics and Evolution

journal homepage: www.elsevier.com/locate/ympev

# Allopatric diversification and evolutionary melting pot in a North African Palearctic relict: The biogeographic history of *Salamandra algira*

Marco Dinis[a], Khaled Merabet[b], Fernando Martínez-Freiría[a], Sebastian Steinfartz[c], Miguel Vences[c], James D. Burgon[d], Kathryn R. Elmer[d], David Donaire[e], Arlo Hinckley[f], Soumia Fahd[g], Ulrich Joger[h], Adnane Fawzi[i], Tahar Slimani[i], Guillermo Velo-Antón[a,*]

[a] CIBIO/InBIO, Centro de Investigação em Biodiversidade e Recursos Genéticos da Universidade do Porto, Instituto de Ciências Agrárias de Vairão, R. Padre Armando Quintas n° 7, 4485-661 Vairão, Portugal
[b] Laboratoire de Recherche en Ecologie et Environnement, Faculté des Sciences de la Nature et de la Vie, Université de Bejaia, 06000 Bejaia, Algeria
[c] Zoological Institute, Braunschweig University of Technology, Mendelssohnstr. 4, 38106 Braunschweig, Germany
[d] Institute of Biodiversity, Animal Health & Comparative Medicine, College of Medical, Veterinary & Life Sciences, University of Glasgow, Glasgow G12 8QQ, UK
[e] Asociación Herpetológica Fretum Gaditanum, Calle Mar Egeo 7, Jerez de la Frontera, Spain
[f] Conservation and Evolutionary Genetics Group, Estación Biológica de Doñana (EBD-CSIC), Avda. Americo Vespucio, 26, 41092 Sevilla, Spain
[g] Equipe de Recherche Ecologie, Systématique, Conservation de la Biodiversité, Département de Biologie, Faculté des Sciences, Université Abbdelmalek Essaâdi, Tétouan, Morocco
[h] State Museum of Natural History, Pockelsstr. 10, 38106 Braunschweig, Germany
[i] Faculty of Sciences Semlalia, Laboratory Biodiversity and Ecosystem Dynamics, Cadi Ayyad University, P.O. Box 2390, 40000 Marrakesh, Morocco

ARTICLE INFO

*Keywords:*
Allopatric divergence
Biogeography
Melting pot
North Africa
Palearctic relict
Salamander

ABSTRACT

North Africa is a climatically and topographically complex region with unique biotic assemblages resulting from the combination of multiple biogeographic realms. Here, we assess the role of climate in promoting intra-specific diversification in a Palearctic relict, the North African fire salamander, *Salamandra algira*, using a combination of phylogenetic and population genetic analyses, paleoclimatic modelling and niche overlap tests. We used mitochondrial DNA (*Cyt-b*), 9838 ddRADseq loci, and 14 microsatellite loci to characterize patterns of genetic diversity and population structure. Phylogenetic analyses recover two major clades, each including several lineages with mito-nuclear discordances suggesting introgressive patterns between lineages in the Middle Atlas, associated with a melting pot of genetic diversity. Paleoclimatic modelling identified putative climatic refugia, largely matching areas of high genetic diversity, and supports the role of aridity in promoting allopatric diversification associated with ecological niche conservatism. Overall, our results highlight the role of climatic microrefugia as drivers of populations' persistence and diversification in the face of climatic oscillations in North Africa, and stress the importance of accounting for different genomic regions when reconstructing biogeographic processes from molecular markers.

## 1. Introduction

North Africa is a climatically and topographically complex region, characterized by Mediterranean climate in the north and arid Saharan climate in the south. Its location at the intersection of distinct biogeographic regions produces a unique species composition (Dobson and Wright, 2000). For Mediterranean lineages in particular, aridity has been a main driver of population fragmentation and subsequent divergence (Cosson et al., 2005), especially from the mid-Pliocene to the Pleistocene when the region regularly experienced alternating humid and hyper-arid phases (Quezel and Barbero, 1993).

Two predominant biogeographic patterns can be observed for Mediterranean species in North Africa. The first is a dual role of mountain systems (especially the Rif and Atlas mountains) as both geographical barriers (e.g. Veríssimo et al., 2016; Martínez-Freiría et al., 2017) and climatic refugia (e.g. Beukema et al., 2010; Barata et al., 2012; Nicolas et al., 2015; Freitas et al., 2018). The second, is a tendency for intraspecific divergence along a west-east axis (e.g. Beukema et al., 2010; Velo-Antón et al., 2012; Stuckas et al., 2014; Beddek et al., 2018), likely associated with historical marine transgressions into river valleys (e.g. Veith et al., 2004) or with periods of climatic fluctuations ranging from humid to hyper-arid conditions

* Corresponding author.
*E-mail address:* guillermo.velo@cibio.up.pt (G. Velo-Antón).

https://doi.org/10.1016/j.ympev.2018.10.018
Received 29 May 2018; Received in revised form 11 October 2018; Accepted 11 October 2018
Available online 12 October 2018
1055-7903/ 

(Cosson et al., 2005). Both of these patterns are consistent with a predominantly allopatric model of diversification, in which ecological niche conservatism would promote vicariance as climatic oscillations created recurrent barriers of unsuitable environmental conditions between conspecific populations.

Recent phylogenomic data have confirmed a sister-group relationship between the widely distributed European fire salamander *S. salamandra* and the north African *S. algira* (Rodríguez et al., 2017). This supports a colonization of North Africa from the Iberian Peninsula during the Messinian Salinity Crisis (MSC) via the Gibraltar land bridge (5.96–5.33 million years ago, [Mya]; Duggen et al., 2003), or a post-MSC colonization during the Messinian-Pliocene transition across the Alborán volcanic archipelago (~7–3 Mya), far east of the Strait of Gibraltar, which formed a land-bridge connection between SE Iberia to the Eastern Rif and facilitated taxa exchange between North Africa and Southern Europe (Booth-Rea et al., 2018). *Salamandra algira* occurs from the Tingitana peninsula in Morocco to the Annaba region in eastern Algeria, with a patchy distribution mostly confined to mountain ranges up to an elevation of 2455 m above sea level. Four subspecies are recognized: *S. a. tingitana* (Donaire-Barroso and Bogaerts, 2003) occupying the north-western Rif; *S. a. splendens* (Beukema et al., 2013), extending into the south-central Rif, possibly including an isolated population in the Middle Atlas; *S. a. spelaea* (Escoriza and Comas, 2007), restricted to a small range in the Beni Snassen massif; and *S. a. algira* (Bedriaga, 1883), apparently restricted to eastern Algeria, with unconfirmed records from western Algeria (Fig. 1). Previous phylogeographic studies using mitochondrial DNA have confirmed the validity of the four subspecies and identified two main clades: a western clade including *S. a. tingitana* and *S. a. splendens*; and an eastern clade including *S. a. spelaea* and *S. a. algira* (Ben Hassine et al., 2016; Merabet et al., 2016). The divergence of these two main clades is estimated in ~3.6 Mya, at the start of a cyclic period of climatic and vegetational fluctuations (Beukema et al., 2010). Similar to other vertebrates (e.g. Velo-Antón et al., 2012; Stuckas et al., 2014), the main biogeographic barrier promoting isolation between these clades is the arid lower Moulouya river basin, as expected for an amphibian species of northern Palearctic origin in North Africa, which is mainly limited by aridity (Escoriza et al., 2006). Divergence within each major clade of *S. algira* may have been associated with periods of climatic fluctuations in North Africa, with phases of persisting aridity imposing vicariance in mountain refugia (Beukema et al., 2010; Ben Hassine et al., 2016). The two subspecies of the western clade are distributed on either side of a contact zone in the Oued (River) Laou (Fig. 1). Likewise, strong geographic structure is also evident within subspecies, as *S. a. tingitana* is divided into three sublineages (Dinis and Velo-Antón, 2017), and *S. a. splendens* also shows geographic structuring, with one sublineage occurring in the Western and Central Rif and another in the Middle Atlas (Beukema et al., 2010).

As an amphibian of Mediterranean origin, *S. algira* is expected to be reliant on the availability of Mediterranean humid habitats with dense vegetation or rock crevices and surface water for reproduction (but see Donaire-Barroso and Bogaerts, 2016; Dinis and Velo-Antón, 2017 on viviparity of *S. algira*). These habitats, however, are sparsely distributed in North Africa, explaining the heavily fragmented and mostly mountainous distribution of this species. Given this relatively restricted ecological tolerance, past climatic oscillations should have played a significant role in the evolutionary history of this species, shaping its distribution and patterns of genetic diversity. Currently our phylogeographic understanding of *S. algira* is limited by reliance mostly on mitochondrial DNA sequence information.

Here, we reconstruct the biogeographic history of *S. algira*, the only terrestrial African salamander, by integrating molecular analyses from multiple independent markers with paleoclimatic modelling. Specifically, we aim to (a) clarify the geographic structure of genetic diversity in *S. algira* and its history of diversification using a combination of mitochondrial DNA, ddRADseq loci and microsatellites; (b) assess the importance of climatic variability in shaping the past and present distribution of *S. algira* and identify potential centres of subspecific diversification using paleoclimatic models; and (c) estimate the degree of ecological niche divergence between sublineages and its role in the evolutionary differentiation within the species.

## 2. Material and methods

### 2.1. Laboratory work and data treatment

Genomic DNA was extracted from toe/tail clips using the Macherey-Nagel NucleoSpin® Tissue kit following manufacturer's instructions for all samples. Two datasets resulting from our field expeditions were combined for mitochondrial DNA (mtDNA) based analysis (Table S2.1). A fragment of the mitochondrial cytochrome *b* gene (*Cyt-b*) was selected based on previous available data. DNA extractions and *Cyt-b* amplification and sequencing were performed for dataset one (ca. 314 bp fragment) as described in Merabet et al. (2016), and for dataset two (91 samples, ca. 1049 bp fragment) as described in Beukema et al. (2016). All further available *Cyt-b* sequences for *S. algira* were

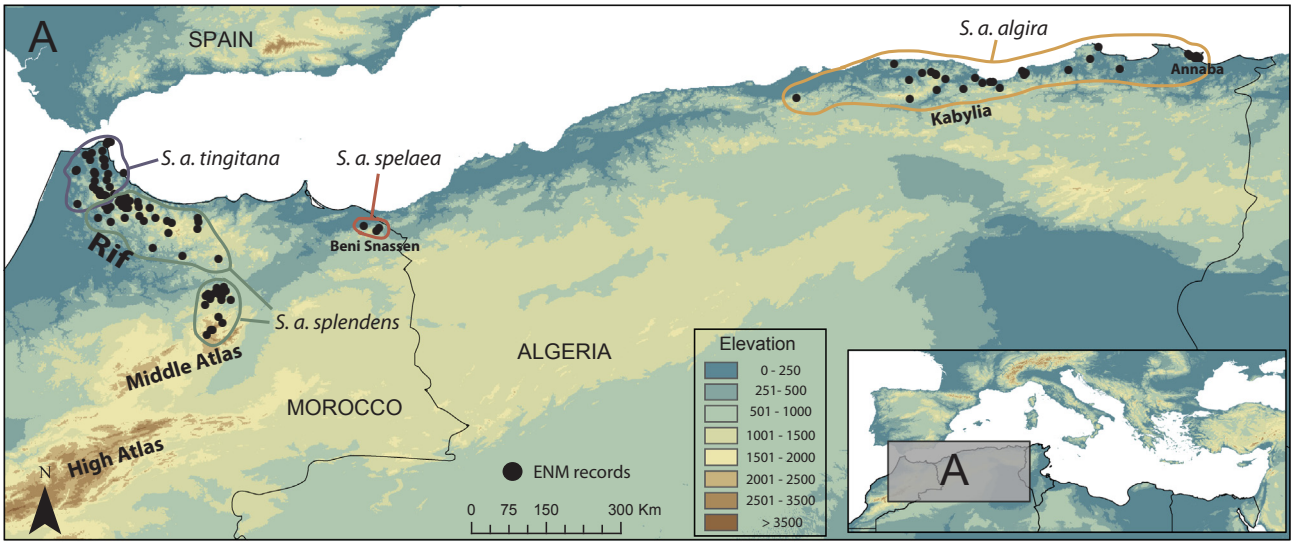


**Fig. 1.** (a) Distribution of *Salamandra algira* records used for paleoclimatic models and niche overlap tests. Polygons depicting the distribution of *S. algira* subspecies and elevation are represented. Small inset shows the location of the study area in the Mediterranean Basin.

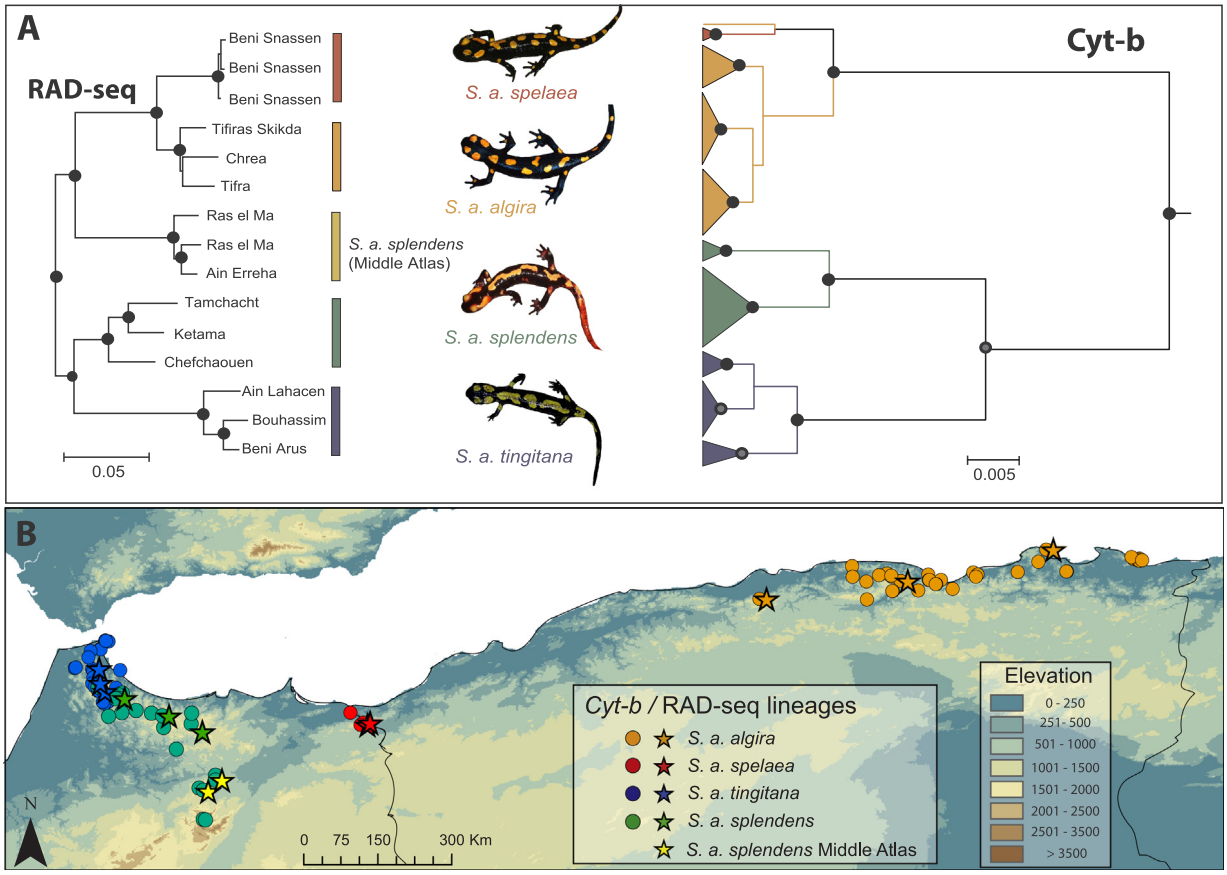


**Fig. 2.** (a) Bayesian phylogenetic trees for *Salamandra algira* obtained from ddRADseq (left) and *Cyt-b* data (right). Black and filled grey dots on tree nodes represent posterior probabilities higher than 0.99 and 0.95, respectively. (b) Geographic distribution of major ddRADseq (stars) and *Cyt-b* lineages (circles). Elevation is represented in the background. Image credits: Guillermo Velo-Antón (*S. a. tingitana*) and David Donaire (*S. a. algira, S. a. spealaea, S. a. splendens*).

downloaded and used in subsequent analyses (269 samples with 314 bp fragment and 91 samples with 1049 bp fragment; Table S2.1). The final alignment was performed in GENEIOUS 11.1.4 and consisted of 360 *Cyt-b* sequences covering the entire distribution of *S. algira*. Sequences from *S. s. longirostris* were included as outgroup.

Three samples representing each of the major mtDNA clades (*S. a. algira*, *S. a. spelaea*, *S. a. tingitana* and the two clades of *S. a. splendens*) from isolated populations were selected for ddRADseq analysis (Table S2.1, Fig. 2). The ddRADseq library preparation for all samples was as follows (per Recknagel et al., 2015, with modification of Illumina adapters): 1 μg of DNA from each individual was double-digested using the PstI-HF® and AclI restriction enzymes (New England Biolabs); modified Illumina adaptors with unique barcodes for each individual were ligated onto this fragmented DNA; samples were multiplexed; and a PippinPrep used to size-select fragments around a tight selection of 383 bp (range: 350–416 bp) based on the fragment-length distribution identified using a 2200 TapeStation instrument (Agilent Technologies). Finally, enrichment PCR was performed to amplify the library using forward and reverse RAD primers. Sequencing was conducted on an Illumina NextSeq™ 500 platform at Glasgow Polyomics to generate paired-end reads 75 bp in length. Raw sequence reads were quality checked using FASTQC v.0.11.3 (Andrews, 2010). Samples were de-multiplexed, Illumina adaptors and barcodes removed, and reads truncated to 60nt using STACKS v.1.44 (Catchen et al., 2011). Given the lack of a reference genome, reads were assembled de novo in STACKS. The minimum number of identical raw reads required to create a stack was set to six (other settings left on default). A whitelist of all loci containing 1–5 SNPs was then generated using custom scripts in R. Samples were then filtered through the STACKS Populations pipeline as a single population, with whitelisted loci retained if they were present in ≥75% of samples, had a minimum individual stack depth of 10, a maximum observed heterozygosity of 0.5, and a minimum minor allele frequency of 0.05. Data were exported in Phylip format, including all variable sites encoded using IUPAC notation.

A total of 14 microsatellite markers developed for *S. salamandra* and previously tested in *S. algira* (Steinfartz et al., 2004; Hendrix et al., 2010; Table S2.2.1) were amplified for datasets one and two (208 individuals successfully genotyped). PCR reactions contained a total volume of 10–11 μl: 5 μl of Multiplex PCR Kit Master Mix (QIAGEN, Valencia, CA, USA), 3 μl of distilled $H_2O$, 1 μl of primer multiplex mix and 1–2 μl of DNA extract (~50 ng/μl). Forward primers were fluorescently labelled (6-FAM, VIC, NED or PET), and reverse primers for dataset one were modified with a "PIG-tail" (GTTT) at the 5' end. Multiplex panels and PCR conditions are described in Tables S2.2.1 and S2.2.2. All allele scoring was performed using GENEMAPPER version 4.0 (Applied Biosystems), and 50% of dataset one (including all alleles found in the dataset) was re-genotyped under dataset two conditions for use as a calibration measure to merge the two datasets.

### 2.2. Phylogenetic analysis

Bayesian phylogenetic analyses of mtDNA were conducted in BEAST v1.7.5 (Drummond et al., 2012). JMODELTEST v.2.1.4 (Darriba et al., 2012) was used to test for the best fitting model of nucleotide substitution for *Cyt-b* (HKY + I), under the Bayesian Information Criterion (BIC). A lognormal relaxed clock and a coalescence constant size model were used as tree priors. Markov Chain Monte Carlo (MCMC) analyses were run in three independent runs of 100 million generations, with a sampling frequency of 10,000 generations. Parameter convergence was verified by examining the effective sample sizes (ESSs) using TRACER

v1.7. After discarding 10% trees as burn-in, the remaining trees were used to obtain the subsequent maximum clade credibility summary tree with posterior probabilities for each node using TREEANNOTATOR. The resulting consensus tree was visualized on FIGTREE (http://tree.bio.ed.ac.uk/software/figtree).

Initial phylogenetic analysis of the concatenated ddRADseq data was performed in RAXML (raxmlHPC; Stamatakis, 2014), using a GTRCAT nucleotide substitution model (without rate heterogeneity) and 1000 bootstrap replicates. Following this, Bayesian analyses were performed in BEAST 2.4.2 (Bouckaert et al., 2014). A BEAST xml file was generated using BEAUTI 2.4.2. The best fitting evolutionary model inferred by BIC in JMODELTEST 2.1.10 was the transversion model (TVM). As BEAST2 only has four base substitution models, which do not include TVM, a GTR substitution model with the alpha gamma rate parameter fixed at one was selected as closest approximation. A relaxed clock (log normal) was used, with all other parameters left on default settings. A MCMC chain of 10 million generations was run (10% burn-in) with tree and parameter estimates sampled every 1000 MCMC generations. Based on this, two prior operators were adjusted: the YuleModelTreeScaler scale factor was set to 0.932 and the size of the YuleModelSubtreeSlide decreased to 0.046. The analysis was then re-run for 100 million generations (10% burn-in). TRACER 1.6.0 (Drummond and Rambaut, 2007) was used to assess chain convergence and a maximum clade credibility tree generated using TREEANNOTATOR 2.4.2.

### 2.3. Spatial patterns of genetic structure and diversity

MICRO-CHECKER 2.2.3 (Van Oosterhout et al., 2004) was used to test microsatellite data for null alleles and allele dropout. Samples from the same locality were grouped into a priori populations for the purposes of testing Hardy–Weinberg Equilibrium (HWE) and Linkage Disequilibrium (LD; assignment of samples to localities on Table S2.1). Each microsatellite locus was tested for HWE and LD using a Markov Chain method with 10,000 dememorization steps and 1000 batches of 10,000 iterations per batch as implemented on GENEPOP 4.2 (Rousset, 2008). Bonferroni correction (Rice, 1989) was applied to account for multiple comparisons.

A Bayesian assignment test based on the full microsatellite dataset was used to infer the number of genetic demes present in our sample, as implemented in STRUCTURE 2.3.1 (Pritchard et al., 2000). One million iterations were performed, with a burn-in period of 100,000, and applying an admixture model with correlated allele frequencies and no prior information on sample population membership. The program was run with a number of clusters (K) ranging from 1 to 20, with 10 iterations per value of K. The most likely value for K was estimated by the highest value of log probability of data L(K) (Falush et al., 2003), and D(K), a measure based on the second order rate of change in L(K) (Evanno et al., 2005).

To visualize the geographic distribution of genetic diversity, metrics of genetic diversity were spatially interpolated. Observed heterozygosity (Ho) and allelic richness (Ar) were calculated from a subset of the microsatellite dataset (70 individuals from 14 localities; 5 individuals/locality; Table S2.3). Ho was calculated on GENALEX 6.5 (Peakall and Smouse, 2012) and Ar was calculated using the R package *diveRsity* (Keenan et al., 2013). Nucleotide diversity ($\pi$) values were calculated for *Cyt-b* by pooling samples contained in a buffer with a radius of 0.4 decimal degrees (~45 km). Nucleotide diversity was calculated independently for each major mitochondrial lineage to avoid artefacts resulting from sampling multiple lineages near the *tingitana/splendens* contact zone. Genetic diversity metrics were then interpolated by generating a continuous surface by kriging interpolation (Oliver and Webster, 1990), implemented in the 'Geostatistical Analyst' extension of ARCMAP 10.1 (ESRI, 2012).

### 2.4. Paleoclimatic models

A database of geo-referenced occurrence records was compiled, including all previously published records, as well as previously unpublished records resulting from our own field expeditions (Fig. 1; Table S2.1). The final database contained 152 unique occurrence records. Potential sampling bias was handled by reducing the level of clustering of the data (Text S1.1).

Five slightly correlated variables ($R < 0.7$; Table S2.4) were obtained from Worldclim (http://www.worldclim.org; Hijmans et al., 2005) for the present as well as for the Mid-Holocene (~6K years ago), Last Glacial Maximum (LGM; ~ 20K) and Last Inter-Glacial (LIG; ~ 120K), representing climatic extremes during the Pleistocene climatic oscillations. These variables were clipped to a study area defined by a 200 km buffer around *S. algira*'s known distribution (Text S1.2). Ecological niche-based models were created at three levels: (a) for the entire species; (b) for each major clade identified by *Cyt-b*; and (c) for each major clade identified by ddRADseq. For levels (b) and (c), records were assigned to their respective clades based on information from phylogenetic trees. Records for which phylogenetic information on lineage membership was unavailable were included when geographical location allowed unambiguous clade assignment, and removed otherwise. For level (b), records without phylogenetic information located near the contact zone were assigned to *S. a. tingitana* or *S. a. splendens* by performing a spatial interpolation of available mitochondrial data, using a modified kriging method implemented in the R package *Phylin* (Text S1.3; Tarroso et al., 2015).

The maximum entropy technique, as implemented in MAXENT (Phillips et al., 2006) has been shown to perform well with low sample sizes (Hernandez et al., 2006), and was therefore used to develop niche-based models based on present climate and projections to past climatic conditions. To assess model parameterization (Merow et al., 2013), different types of features and regularization multiplier values were tested (Fig. S3.1). Final models were created using linear and quadratic features and a regularization multiplier of 0.5. Each model was created by running 50 bootstrap replicates, each one setting aside 30% of the available presence points for model testing. Forecasts of suitability were created by averaging the 50 replicates for each taxon.

Model accuracy was assessed using the Area Under the Curve (AUC) of the Receiver Operating Characteristic (ROC) plots for the training and testing datasets. Standard deviation plots of model replicates were also taken into consideration when assessing model performance. The importance of environmental variables for each model was determined by the average percentage of contribution (Phillips et al., 2006). Response curves for the most important variables were visually inspected to detect differences in ecological requirements among taxa (e.g. Martínez-Freiría et al., 2008). Average consensus models of the replicates were projected to the area of the full species' distribution in the present to identify areas of overlap between subspecies, as well as to the same area under past conditions to identify areas of past climatic suitability and to evaluate the responses of taxa to past climatic oscillations at the regional scale. Projections used the Fade By Clamping option, to reduce the error associated with projecting to environmental conditions beyond the range used for training. To avoid biases associated with selection of thresholds for model classification, areas that are consistently suitable across all time periods were identified using a fuzzy approach (e.g. Gutiérrez-Rodríguez et al., 2017). Model predictions for all time periods were upscaled to the coarsest resolution ($5 \times 5$ km). Fuzzy intersections between all time periods were calculated independently for each GCM using the Fuzzy Overlay approach with the "AND" function on ARCMAP, which incorporates information from all projections while attributing less weight to individual projections.

### 2.5. Niche overlap tests

The R package *ecospat* (Di Cola et al., 2017) was used to quantify the degree of ecological niche overlap and to test the contrasting hypotheses of niche conservatism versus niche divergence between clades. Niche overlap between each pair of clades was calculated independently for groups defined on levels (b) and (c), and niche equivalency and similarity tests were performed for all pairs. Niche equivalency tests determine whether niche overlap is constant when randomly reallocating the occurrences of both groups among their respective ranges, while niche similarity tests decouple the effects of differential habitat selection versus habitat availability on the niche overlap between lineages, by taking into account information on the geographic availability of environmental conditions (Warren et al., 2008; Broennimann et al., 2012). An area defined by a 200 km buffer around the species' distribution was used as background area. A total of 100 pseudoreplicates were generated for each test.

## 3. Results

### 3.1. Phylogenetic analyses

The *Cyt-b* tree identified two major clades: a western clade (*sensu* Ben Hassine et al., 2016) comprising two monophyletic groups corresponding to the subspecies *S. a. tingitana* (NW Moroccan Rif) and *S. a. splendens* (SW and Central Rif and Middle Atlas), and an eastern clade (*sensu* Ben Hassine et al., 2016) comprising *S. a. spelaea* in the Moroccan Beni Snassen massif and *S. a. algira* in Algeria; Figs. 2 and S3.2). Delimitation of subspecies within the eastern clade was hindered by the paraphyletic status of *S. a. algira*, due to a sister-group relationship between the westernmost Algerian population from Chrea and *S. a. spelaea* from Beni Snassen (Fig. S3.2), possibly caused by insufficient phylogenetic information in this short mtDNA segment. *Salamandra a. tingitana* and *S. a. splendens* are further subdivided into three (mostly separated by the boundaries of river Martil) and two (southwestern/central Rif and Middle Atlas) monophyletic groups, respectively. Major nodes, except for the divergence of *S. a. tingitana* sublineages, were highly supported (PP $>$ 0.95; Fig. S3.2).

The ddRADseq tree based on 9838 RAD-loci (15,859 SNPs) identified two major clades with high node support (PP $>$ 0.95): one clade included two sister groups corresponding to *S. a. tingitana* and the Rif populations of *S. a. splendens*. The other clade contained the second lineage of *S. a. splendens*, from the Middle Atlas, which was the sister lineage to a *S. a. spelaea* and *S. a. algira* grouping (Figs. 2 and S3.3).

### 3.2. Patterns of spatial genetic structure and diversity

For the microsatellite dataset, no null alleles or allele dropout (99% confidence interval) nor significant deviations from Hardy Weinberg equilibrium or evidence of Linkage Disequilibrium were observed. Both L(K) and D(K) identified K = 7 as the best number of clusters for the Structure analysis (Fig. S3.4), which mostly corresponded to discrete geographic locations (Fig. 3). In the Moroccan Rif, three clearly delimited clusters are found, corresponding to the localities of Ceuta and Amsa, and a third cluster grouping all remaining NW Rif localities, even across the contact zone between *S. a. tingitana* and *S. a. splendens* in Oued Laou. Localities in the SW and Central Rif show extensive admixture and are not assigned to any particular cluster. Two clusters correspond roughly to the Algerian regions of Kabylia and Annaba, though some admixture occurs between the two. The remaining two clusters correspond to Beni Snassen and the Middle Atlas populations (Fig. 3).

### 3.3. Spatial interpolations

The highest values of allelic richness and heterozygosity for microsatellite loci occur in the Middle Atlas, Annaba and the western Rif, while the lowest occur in Beni Snassen and Dar Chaoui (Fig. 4a; Table S2.3). Interpolations of nucleotide diversity ($\pi$) identified distinct geographic patterns for each group: a west-east cline for *S. a. tingitana*, with the lowest $\pi$ in the eastern localities of Ceuta and Amsa (Fig. 4b; Table S2.5); a north-south cline for *S. a. splendens*, with the highest values found near its contact zone with *S. a. tingitana* and the lowest in the southern Rif (Fig. 4c; Table S2.5). In the eastern clade, the highest values occurred in Kabylia, while in the rest of the clade, distribution was predicted to have much lower diversity overall (Fig. 4d; Table S2.5).

### 3.4. Paleoclimatic models

Overall, accuracy was high for all models (Table 1). Wet-season precipitation was the most important variable for all models, with the models for *S. a. splendens* (mtDNA-based) and the eastern clade (ddRADseq-based) importantly affected by other variables too, particularly maximum temperature of the warmest month (Table 1). Suitability for all models was positively correlated with wet-season precipitation and negatively correlated with lower maximum temperature values (Fig. S3.5). All models predicted current suitable areas predominantly in the Rif and northeast Algeria, and low suitability in Beni Snassen (Fig. S3.6). Models for *S. a. splendens* (mtDNA) and the eastern clade (ddRADseq) predicted suitable areas in the Middle Atlas (Fig. S3.6).

Predictions of climatically stable areas were similar for all GCMs (Figs. 5, S3.7). The overlay of species model and projections depicted areas with high stable climatic suitability in the north-western Rif and eastern Kabylia (Figs. 5a, S3.7). On the overlays for the mtDNA-based models, stable high-suitability areas were identified for *S. a. tingitana* near Ceuta; for *S. a. splendens* in the south-western and central Rif; and for the eastern clade in Kabylia (Figs. 5b, S3.7). For the ddRADseq-based western clade, stable high-suitability areas were identified in the north-western Rif, restricted to the north of Oued Laou; while for the eastern clade, stable high-suitability areas were identified in the southwestern and central Rif and in Kabylia (Figs. 5c, S3.7).

Niche overlap was consistently low (D $<$ 0.21). Nonetheless, niche equivalency tests failed to reject the null hypothesis of niche equivalency among all lineage pairs. Similarly, the only significant similarity test (between *S. a. tingitana* and *S. a. splendens*) was associated with a value of niche overlap greater than the distribution of pseudoreplicates (D = 0.202), indicating that niches of the two subspecies are more similar than expected given the available environmental conditions for each. All other similarity tests were non-significant, and thus inconclusive regarding niche similarity (Table 2).

## 4. Discussion

### 4.1. Biogeographic affinities of Salamandra algira

Species responses to Pleistocene glacial and interglacial periods are idiosyncratic and shaped by their biogeographic affinities (Stewart et al., 2010). Responses of *S. algira* were similar to other species located on the southernmost limits of their climatic range (e.g. de Pous et al., 2013; Martínez-Freiría et al., 2015, 2017), with range contractions during the LIG and, to a lesser extent, the Mid-Holocene, and expansions during the LGM (Fig. S3.6). Populations at southernmost climatic margins might be susceptible to an increase of temperature and aridity, contracting ranges to mountains, while range expansions to the lowlands should occur during mild and humid periods.

The lack of evidence for niche divergence (reflected in the failure to reject niche equivalency and similarity) supports previous assertions that all *S. algira* lineages have similar ecological (bioclimatic) requirements. Differences between lineages (reflected in the low values of niche overlap) are therefore more likely related to differences in local

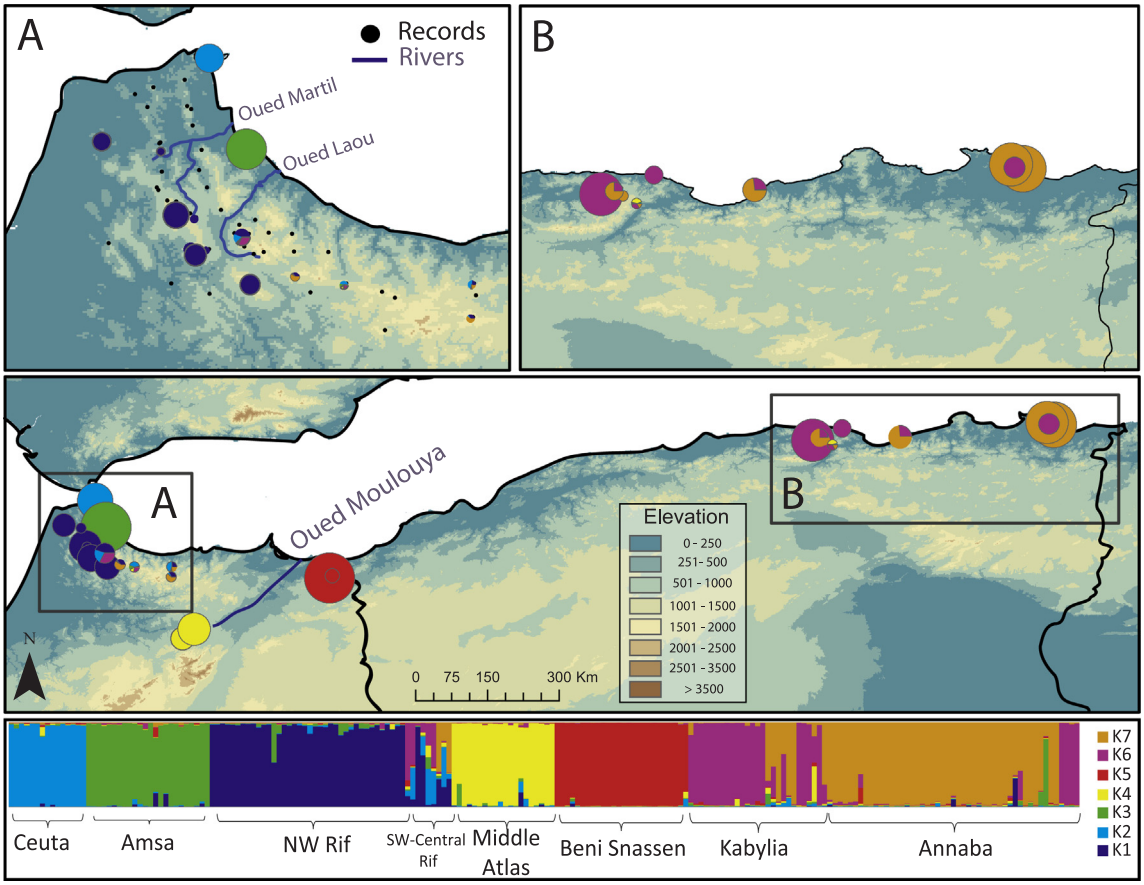


**Fig. 3.** Geographic distribution of demes of *Salamandra algira* population structure in North Africa diagnosed using microsatellite data. Circle size represents relative sample size for the locality. (a) Close up of *S. algira* population structure in the Moroccan Rif. Major rivers and available occurrence records are also represented. (b) Close up of *S. algira* population structure in north-eastern Algeria. Bottom panel: Plot of STRUCTURE results. Localities or regions associated with each deme are described below the plot.

availability of habitats rather than to adaptive divergence in habitat selection (Ben Hassine et al., 2016), with models for all lineages associated with high levels of wet-season precipitation. This variable is expected to have a dual role in the delimitation of the distribution of *S. algira*: first, a causal positive relationship exists between precipitation and vegetation productivity, and *S. algira* can benefit from the microclimatic buffer effects of vegetation (Escoriza and Ben Hassine, 2014); second, high precipitation likely favours *S. algira* larviparous populations directly by providing surface water for reproduction.

### 4.2. Allopatric diversification in Salamandra algira

Allopatric divergence associated with topographic and climatic barriers and niche conservatism have been the major drivers of intraspecific diversification in *S. algira,* as inferred from non-overlapping (mtDNA) or only partially overlapping (ddRADseq) stable areas of high climatic suitability for each major lineage, with no evidence for niche divergence across lineage pairs. This is in line with the predominantly vicariant mode of speciation in salamanders, which often show deeply divergent intra-specific lineages, and spatially structured genetic diversity (e.g. Martínez-Solano et al., 2007; Veith et al., 2008; Beukema et al., 2016; Salvi et al., 2016). Allopatric diversification mediated by Pleistocene climatic fluctuations has also been identified as the main driver of intra-specific diversification in other North African species (e.g. Anadón et al., 2015; Veríssimo et al., 2016; Martínez-Freiría et al., 2017; see also Husemann et al., 2014).

The past distribution of *S. algira* was probably also constrained by non-climatic abiotic and biotic pressures. For instance, factors associated with vegetation and lithology (see Beukema et al., 2010), not detectable by climate-only models, may have constrained distributions more extensively than observable using the biogeographic approach applied here. Also, river systems like the Mouloya, Oued Martil or Oued Laou may have acted as barriers, promoting vicariance. Models based on the ddRADseq results predict partially overlapping stable areas for the eastern and western clades in the Rif, which likely acted as climatic refugia and centres of diversification. This agrees with the well-established role of Moroccan mountain ranges as an important centre of diversification (e.g. Barata et al., 2012; Beukema et al., 2010; Nicolas et al., 2015; Veríssimo et al., 2016; Freitas et al., 2018). It is unclear where the differentiation of the west and east clades took place, but based on their distribution at each side of the Mouluya river basin, it might have started in this area when the ancestors of *S. algira* colonized Africa from the Iberian Peninsula via the archipelago created with the East Alborán volcanic arc (Booth-Rea et al., 2018). The Moulouya basin constitutes a stable low-suitability region on all models; thus, it likely played a later role in maintaining allopatry between the east and west clades, as suggested for other taxa (Escoriza et al., 2006; Beukema et al., 2010; Merabet et al., 2016). Then, subsequent westward and eastward population expansions could occur in the west and east clade, respectively.

Differentiation within the western clade (*S. a. tingitana* - *S. a. splendens*) likely took place in independent climatic refugia in the Rif, as attested by predicted stable areas based on mitochondrial DNA, while diversification in the eastern clade (*S. a spelaea* - *S. a. algira*) was associated with eastward expansion. Species may persist in microclimatic refugia in areas where the regional climate ceases to be suitable (e.g. Worth et al., 2014), but these microrefugia are difficult to detect using ecological models based on climatic predictors with low spatial

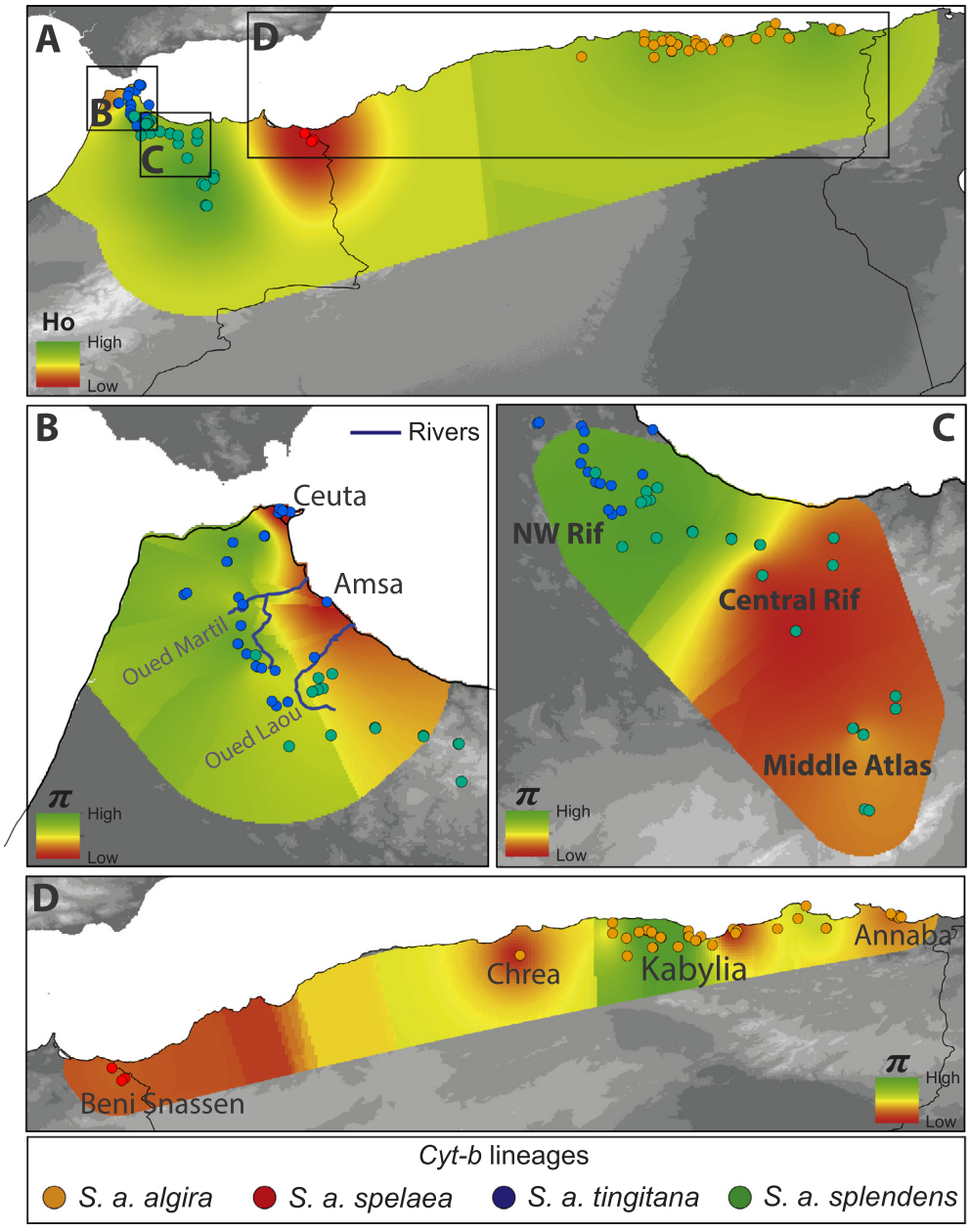


**Fig. 4.** Spatial interpolations of *Salamandra algira* genetic diversity across its distribution in North Africa (a) Observed heterozygosity (b) Nucleotide diversity ($\pi$) for *S. a. tingitana*. (c) Nucleotide diversity for *S. a. splendens*. (d) Nucleotide diversity for the east clade. Observed heterozygosity and nucleotide diversity were calculated from microsatellite and *Cyt-b* data, respectively. Distribution of *Cyt-b* lineages, major river systems of the Rif and names of relevant localities are also represented. The spatial interpolation of allelic richness was very similar to the one for observed heterozygosity, and is not represented. Nucleotide diversity values were interpolated to the area defined by the minimum convex polygon that includes the entire distribution of the lineage.

**Table 1**
Average (and SD) performance metrics and percent contribution of each variable to ecological niche-based models for *Salamandra algira* and its sublineages, as defined by *Cyt-b* and ddRADseq data. N: Sample size; AUC: Area Under the Curve; BIO4: temperature seasonality; BIO5: maximum temperature of warmest month; BIO6: minimum temperature of coldest month; BIO16; precipitation of wettest quarter; BIO18: precipitation of warmest quarter; SAT: *S. a. tingitana*; SAS: *S. a. splendens*. Most important variables are outlined in bold.

| | | N | Performance metrics | | Variable percent contribution | | | | |
|---|---|---|---|---|---|---|---|---|---|
| Species | | | Training AUC | Test AUC | BIO4 | BIO5 | BIO6 | BIO16 | BIO18 |
| | | 112 | 0.933 (0.009) | 0.93 (0.019) | 5.8 (3.5) | 11.8 (3.8) | 4 (1.6) | **73.7 (4.3)** | 4.7 (1.6) |
| *Cyt-b* | **East** | 36 | 0.950 (0.017) | 0.0931 (0.039) | 5.5 (6.9) | 7.9 (4.3) | 3 (3.4) | **81 (8.4)** | 2.6 (2.3) |
| | **SAT** | 30 | 0.974 (0.007) | 0.97 (0.012) | 8.4 (2.7) | 15.5 (5.7) | 7.7 (3.6) | **68.5 (7.6)** | 0.1 (0.2) |
| | **SAS** | 52 | 0.925 (0.013) | 0.912 (0.024) | 0.2 (0.2) | **32.9 (9.3)** | **23.2 (4.3)** | **42.1 (11.0)** | 1.7 (1.5) |
| RADseq | **West** | 63 | 0.964 (0.008) | 0.961 (0.014) | 1.1 (1.3) | 15.5 (4.9) | 2.7 (1.9) | **78.4 (5.8)** | 2.3 (2.2) |
| | **East** | 57 | 0.897 (0.022) | 0.882 (0.035) | 7.2 (5.2) | **27.0 (10.1)** | 4.3 (3.4) | **43.0 (11.1)** | **19.0 (5.3)** |

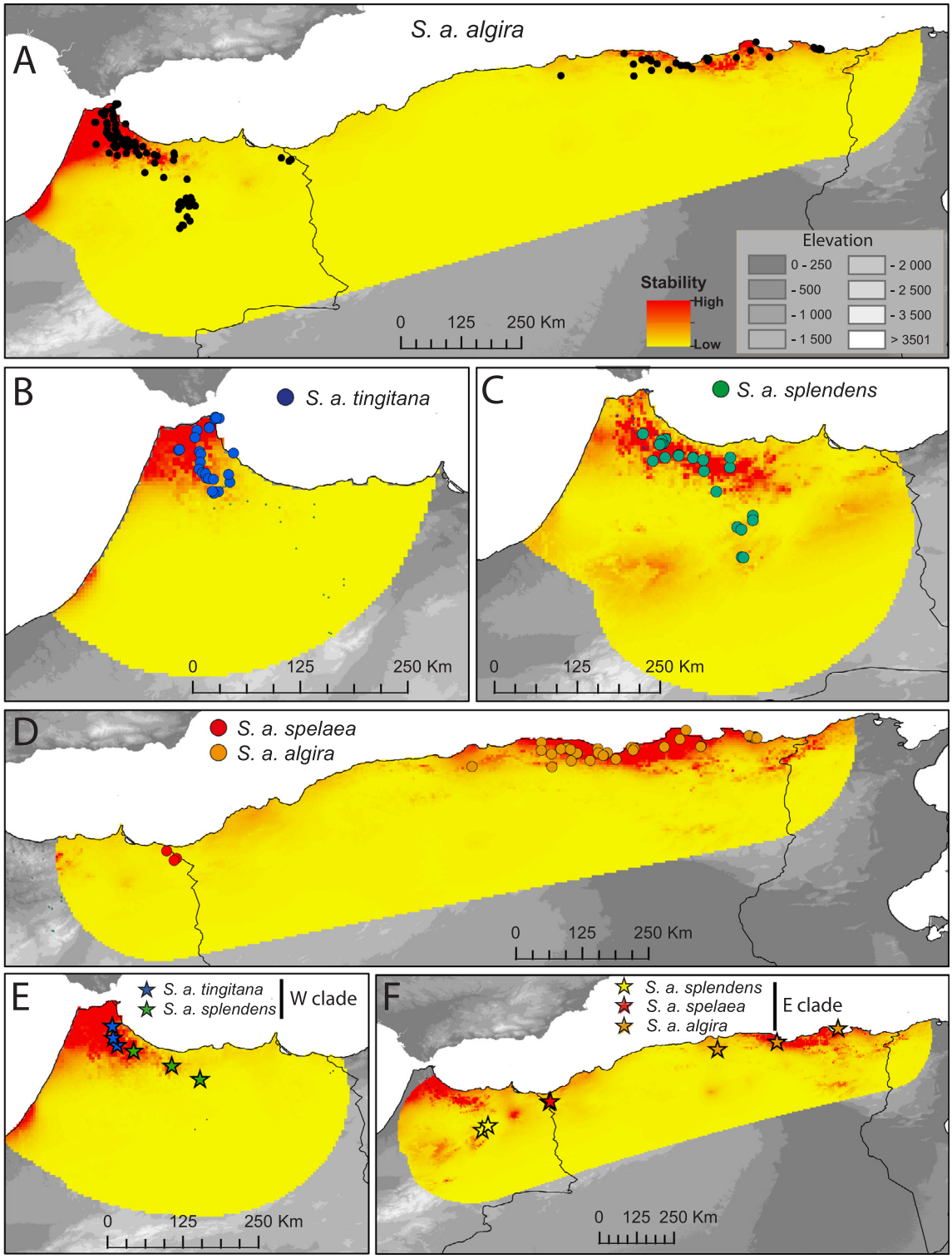


**Fig. 5.** Stable climatically suitable areas derived from fuzzy logic overlay of paleoclimatic models for *Salamandra algira* lineages projected to the present and to three periods in the past (LIG, MidHol and LGM), using MidHol and LGM predictions derived from the CCSSM4 Global Circulation Model. Projection areas correspond to the calibration areas used for model training. (a) For the entire species. (b) For *S. a. tingitana* identified by *Cyt-b*. (c) For *S. a. splendens* identified by *Cyt-b*. (d) For the eastern clade (*S. a. spelaea* and *S. a. algira*) identified by *Cyt-b*. (e) For the western clade (*S. a. tingitana* and *S. a. splendens*) identified by ddRADseq. (f) For the eastern clade (*S. a. spelaea* and *S. a. algira*) identified by ddRADseq.

resolution (e.g. Hijmans et al., 2005). The lack of climatic stability in the Beni Snassen massif, where the highly localized and microclimate-dependent *S. a. spelaea* is found (Escoriza and Ben Hassine, 2014), suggests that this area could have acted as a microrefugium for the species. On the other hand, the inference of a single stable climatic area in Kabylia, coupled with the extensive admixture found in Algerian populations, supports previous assertions of connectivity between populations driven by climatic stability in the area (Ben Hassine et al., 2016; Merabet et al., 2016; Bouzid et al., 2017). However, the existence of intermediate populations in west Algeria (Ben Hassine et al., 2016)

**Table 2**
Niche overlap, and equivalency and similarity test (p-value) between all pairs of *Salamandra algira* lineages, as defined by *Cyt-b* and ddRADseq. Non-significant p-values ($p > 0.05$) indicate that niche equivalency or similarity could not be rejected. P-values in bold are significant, yet indicate pairs of lineages more similar than expected, due to niche overlap being greater than expected by chance. D: niche overlap (Schoener's D).

| | Comparisons | D | Equivalency | Similarity | |
|---|---|---|---|---|---|
| | | | | A- > B | B- > A |
| mtDNA | *S. a. tingitana* – *S. a. splendens* | 0.202 | 0.96 | **0.04** | **0.03** |
| | *S. a. tingitana* – East clade | 0.045 | 1 | 0.208 | 0.307 |
| | *S. a. splendens* – East clade | 0.111 | 1 | 0.218 | 0.168 |
| ddRADseq | East – West | 0.089 | 1 | 0.456 | 0.416 |

makes further sampling necessary to disentangle whether paleoclimatic model predictions of unsuitable habitat in Beni Snassen and Chrea reflect their microrefugial status or an artefact resulting from incomplete sampling of the species' climatic niche.

### 4.3. Cyto-nuclear discordance, the melting pot in the Middle Atlas and contemporary genetic structure

We found a strong cyto-nuclear discordance in the Middle Atlas salamander populations, probably resulting from mitochondrial introgression during population expansion from neighbouring climatically stable areas into this region. In the resulting melting pot of *S. algira* lineages in the Middle Atlas, the high values of genetic diversity reflect contributions from multiple gene pools to local genetic diversity. An early expansion of *S. a. splendens* into the Middle Atlas, followed by a subsequent colonization of the eastern clade, could account for this pattern. While the underlying causes cannot be determined with the data at hand, nuclear DNA has been previously found to cross contact zones faster than mitochondrial DNA in the genus *Salamandra,* possibly due to a combination of male-biased dispersal and selection for traits coded in the nuclear genome (García-París et al., 2003; Pereira et al., 2016), and phylopatry in *S. atra* (Helfer et al., 2012), and *S. salamandra* females (Lourenço et al., 2018) has been suggested.

Microsatellites helped to clarify contemporary patterns of population structure. The genetic distinctiveness of the Middle Atlas and Beni Snassen populations agrees with the predictions of niche models to the present. The Middle Atlas populations are surrounded by unsuitable habitat, including the Moulouya river basin to the east and the region between the Rif and the Middle Atlas to the north. On the other hand, the prediction of Beni Snassen as climatically unsuitable habitat underpins the idea that *S. algira* may be highly reliant on patches of suitable microhabitat conditions (see Ben Hassine et al., 2016) enforcing population isolation. The possible presence of *S. algira* populations in west Algeria leaves open the possibility that the assignment of Beni Snassen to a distinct deme is an artefact resulting from isolation by distance.

## 5. Conclusion

We unravelled the biogeographic processes governing the intraspecific diversification of a North African Palearctic relict. Climatic oscillations promoted allopatric diversification, driven by aridity as a major limiting factor. Major centres of diversification include the Moroccan Rif and in the Algerian region of Kabylia. No reproductive barriers were observed between subspecies that make geographic contact, with continuous gene flow between *S. a. tingitana* and *S. a. splendens* in the Rif Mountains, and past introgression between *S. a. splendens* and a population of the eastern clade, creating a melting pot of genetic diversity in the Middle Atlas via multiple populations expanding into this region. We propose a potential role of microrefugia as drivers of persistence and diversification in the face of climatic oscillations in North Africa. The discordance between different DNA regions highlights the need to evaluate evolutionary and demographic processes for different genomic regions when assessing biogeographic processes resorting to niche-based modelling approaches.

## 6. Data accessibility

Data set of microsatellite genotypes for *Salamandra algira* is available in supplementary material (Table S2.6). GenBank accession numbers for the *cytochrome b* sequences generated in this study are the following: MH986344 - MH986594.

## 7. Author contributions

GV-A, MD, SS, MV and FM-F conceived the study; GV-A, MD, FM-F, SF, KM, DD, AH, UJ, AF and TS performed the sampling; MD, KM, KE and JB performed laboratory work; MD, KE, JB and GV-A analysed the data; MD and GV-A wrote the manuscript with important contributions from co-authors.

## Acknowledgements

We thank Javier Martínez-Medina, Saul Yubero, Francisco Jiménez-Cazalla, Luis García-Cardenete and Wouter Beukema for sharing tissue samples or for help during field work. Acknowledgements are extended to André Lourenço, Paulo Pereira, Julia Männicke, Meike Kondermann and Gaby Keunecke for assistance with laboratory and analytical work. This work was funded by FEDER funds through the Operational Programme for Competitiveness Factors – COMPETE, by National Funds through FCT – Foundation for Science and Technology under the PTDC/BIA-EVF/3036/2012, PTDC/BIA-EVL/28475/2017 and FCOMP-01-0124-FEDER-028325, and a grant from Instituto de Estudios Ceutíes (IEC 2015) to GVA, by the Moroccan-German Program for Scientific Research [PMARS II N °: MA 12/07], by the Hassan II Academy of Sciences and Technics - Morocco (ICGVSA project) and by a Natural Environment Research Council PhD studentship NE/L501918/1 to JB with KRE. GV-A and FM-F are supported by FCT (IF/01425/2014 and SFRH/BPD/109119/2015, respectively). UJ, MV and TS were supported by German Science Ministry (BMBF: 01DH13015). Fieldwork for obtaining tissue samples was done with the corresponding permits from the Moroccan administration (n° 19/2015/HCEFLCD/DLCDPN/DPRN/CFF).

## Appendix A. Supplementary material

Supplementary data to this article can be found online at https://doi.org/10.1016/j.ympev.2018.10.018.

## References

Anadón, J.D., Graciá, E., Botella, F., Giménez, A., Fahd, S., Fritz, U., 2015. Individualistic response to past climate changes: niche differentiation promotes diverging Quaternary range dynamics in the subspecies of *Testudo graeca*. Ecography 38, 956–966.

Andrews, S., 2010, FastQC, Available at: < http://www.bioinformatics.babraham.ac.uk/projects/fastqc/ > .

Barata, M., Perera, A., Martínez-Freiría, F., Harris, D.J., 2012. Cryptic diversity within the Moroccan endemic day geckos *Quedenfeldtia* (Squamata: Gekkonidae): a multidisciplinary approach using genetic, morphological and ecological data. Biol. J. Linn. Soc. 106, 828–850.

Beddek, M., Zenboudji-Beddek, S., Geniez, P., Fathalla, R., Sourouille, P., Arnal, V., Dellaoui, B., Koudache, F., Telailia, S., Peyre, O., Crochet, P.A., 2018. Comparative phylogeography of amphibians and reptiles in Algeria suggests common causes for the east-west phylogeographic breaks in the Maghreb. PloS One 13 (8), e0201218.

Bedriaga, J.V., 1883. Beiträge zur kenntnis der amphibien und reptilien der fauna von Korsika. Archiv. für Naturgeschichte, Berlin.

Ben Hassine, J., Gutiérrez-Rodríguez, J., Escoriza, D., Martínez-Solano, I., 2016. Inferring the roles of vicariance, climate and topography in population differentiation in

*Salamandra algira* (Caudata, Salamandridae). J. Zool. Syst. Evol. Res. 54, 116–126.
Beukema, W., De Pous, P., Donaire-Barroso, D., Bogaerts, S., Garcia-Porta, J., Escoriza, D., Arribas, O.J., El Mouden, E.H., Carranza, S., 2013. Review of the systematics, distribution, biogeography and natural history of Moroccan amphibians. Zootaxa 3661, 1–60.
Beukema, W., De Pous, P., Donaire-Barroso, D., Escoriza, D., Bogaerts, S., Toxopeus, A.G., De Bie, C.A.J.M., Roca, J., Carranza, S., 2010. Biogeography and contemporary climatic differentiation among Moroccan *Salamandra algira*. Biol. J. Linn. Soc. 101, 626–641.
Beukema, W., Nicieza, A.G., Lourenço, A., Velo-Antón, G., 2016. Colour polymorphism in *Salamandra salamandra* (Amphibia: Urodela), revealed by a lack of genetic and environmental differentiation between distinct phenotypes. J. Zool. Syst. Evol. Res. 54, 127–136.
Booth-Rea, G., Ranero, C.R., Grevemeyer, I., 2018. The Alboran volcanic-arc modulated the Messinian faunal exchange and salinity crisis. Scient. Rep. 8 (1), 13015.
Bouckaert, R., Heled, J., Kühnert, D., Vaughan, T., Wu, C.H., Xie, D., Suchard, M.A., Rambaut, A., Drummond, A.J., 2014. BEAST 2: a software platform for Bayesian evolutionary analysis. PLoS Comput. Biol. 10, 1–6.
Bouzid, S., Konecny, L., Grolet, O., Douady, C.J., Joly, P., Bouslama, Z., 2017. Phylogeny, age structure, growth dynamics and colour pattern of the *Salamandra algira algira* population in the Edough Massif, northeastern Algeria. Amphib. Reptil. 38, 461–471.
Broennimann, O., Fitzpatrick, M.C., Pearman, P.B., Petitpierre, B., Pellissier, L., Yoccoz, N.G., Thuiller, W., Fortin, M.J., Randin, C., Zimmermann, N.E., Graham, C.H., 2012. Measuring ecological niche overlap from occurrence and spatial environmental data. Glob. Ecol. Biogeo. 21, 481–497.
Catchen, J.M., Amores, A., Hohenlohe, P., Cresko, W., Postlethwait, J.H., 2011. Stacks: building and genotyping loci de novo from short-read sequences. G3: Genes, Genom. Genet. 1, 171–182.
Cosson, J.F., Hutterer, R., Libois, R., Sarà, M., Taberlet, P., Vogel, P., 2005. Phylogeographical footprints of the Strait of Gibraltar and Quaternary climatic fluctuations in the western Mediterranean: a case study with the greater white-toothed shrew, *Crocidura russula* (Mammalia: Soricidae). Mol. Ecol. 14, 1151–1162.
Darriba, D., Taboada, G.L., Doallo, R., Posada, D., 2012. jModelTest 2: more models, new heuristics and parallel computing. Nat. Methods 9, 772.
Di Cola, V., Broennimann, O., Petitpierre, B., Breiner, F.T., D'Amen, M., Randin, C., Engler, R., Pottier, J., Pio, D., Dubuis, A., Pellissier, L., Mateo, R.G., Hordijk, W., Salamin, N., Guisan, A., 2017. Ecospat: an R package to support spatial analyses and modeling of species niches and distributions. Ecography 40, 774–787.
Dinis, M., Velo-Antón, G., 2017. How little do we know about the reproductive mode in the north African salamander, *Salamandra algira*? Pueriparity in divergent mitochondrial lineages of *S. a. tingitana*. Amphib. Reptil. 38, 540–546.
Dobson, M., Wright, A., 2000. Faunal relationships and zoogeographical affinities of mammals in north-west Africa. J. Biogeogr. 27, 417–424.
Donaire-Barroso, D., Bogaerts, S., 2003. A new subspecies of *Salamandra algira* Bedriaga, 1883 from northern Morocco. Podarcis 4, 84–100.
Donaire-Barroso, D., Bogaerts, S., 2016. Sobre los límites de *Salamandra algira tingitana* Donaire-Barroso & Bogaerts, 2003 vivípara y consideraciones ecológicas. Butll Soc. Cat. Herp. 23, 64–70.
Drummond, A.J., Rambaut, A., 2007. BEAST: Bayesian evolutionary analysis by sampling trees. BMC Evol. Biol. 7, 214.
Drummond, A.J., Suchard, M.A., Xie, D., Rambaut, A., 2012. Bayesian phylogenetics with BEAUti and the BEAST 1.7. Mol. Biol. Evol. 29, 1969–1973.
Duggen, S., Hoernle, K., Van Den Bogaard, P., Rüpke, L., Morgan, J.P., 2003. Deep roots of the Messinian salinity crisis. Nature 422 (6932), 602.
Escoriza, D., Comas, M.D.M., Donaire-Barroso, D., Carranza, S., 2006. Rediscovery of *Salamandra algira* Bedriaga, 1833 from the Beni Snassen massif (Morocco) and phylogenetic relationships of North African *Salamandra*. Amphib. Reptil. 27, 448–455.
Escoriza, D., Comas, M.D.M., 2007. Description of a new subspecies of *Salamandra algira* Bedriaga, 1883 (Amphibia: Salamandridae) from the Beni Snassen Massif (northeast Morocco). Salamandra 43, 77–90.
Escoriza, D., Ben Hassine, J., 2014. Microclimatic variation in multiple *Salamandra algira* populations along an altitudinal gradient: phenology and reproductive strategies. Acta Herpetologica 9, 33–41.
ESRI, 2012, ArcGIS 10.1.
Evanno, G., Regnaut, S., Goudet, J., 2005. Detecting the number of clusters of individuals using the software STRUCTURE: a simulation study. Mol. Ecol. 14, 2611–2620.
Falush, D., Stephens, M., Pritchard, J.K., 2003. Inference of population structure using multilocus genotype data: linked loci and correlated allele frequencies. Genetics 164, 1567–1587.
Freitas, I., Fahd, S., Velo-Antón, G., Martínez-Freiría, F., 2018. Chasing the phantom: biogeography and conservation of *Vipera latastei-monticola* in the Maghreb (North Africa). Amphib. Reptil. 39, 145–161.
García-París, M., Alcobendas, M., Buckley, D., Wake, D.B., 2003. Dispersal of viviparity across contact zones in Iberian populations of fire salamanders (*Salamandra*) inferred from discordance of genetic and morphological traits. Evolution 57, 129–143.
Gutiérrez-Rodríguez, J., Barbosa, A.M., Martínez-Solano, Í., 2017. Integrative inference of population history in the Ibero-Maghrebian endemic *Pleurodeles waltl* (*Salamandridae*). Mol. Phylogenet. Evol. 112, 122–137.
Helfer, V., Broquet, T., Fumagalli, L., 2012. Sex-specific estimates of dispersal show female philopatry and male dispersal in a promiscuous amphibian, the alpine salamander (*Salamandra atra*). Mol. Ecol. 2, 4706–4720.
Hendrix, R.S., Hauswaldt, J., Veith, M., Steinfartz, S., 2010. Strong correlation between cross-amplification success and genetic distance across all members of "True Salamanders" (Amphibia: Salamandridae) revealed by *Salamandra salamandra*-specific microsatellite loci. Mol. Ecol. Resour. 10, 1038–1047.
Hernandez, P.A., Graham, C., Master, L.L., Albert, D.L., 2006. The effect of sample size and species characteristics on performance of different species distribution modeling methods. Ecography 29, 773–785.
Hijmans, R.J., Cameron, S.E., Parra, J.L., Jones, P.G., Jarvis, A., 2005. Very high resolution interpolated climate surfaces for global land areas. Int. J. Climatol. 25, 1965–1978.
Husemann, M., Schmitt, T., Zachos, F.E., Ulrich, W., Habel, J.C., 2014. Palaearctic biogeography revisited: evidence for the existence of a North African refugium for Western Palaearctic biota. J. Biogeogr. 41, 81–94.
Keenan, K., Mcginnity, P., Cross, T.F., Crozier, W.W., Prodöhl, P.A., 2013. DiveRsity: an R package for the estimation and exploration of population genetics parameters and their associated errors. Methods Ecol. Evol. 4, 782–788.
Lourenço, A., Antunes, B., Wang, I.J., Velo-Antón, G., 2018. Fine-scale genetic structure in a salamander with two reproductive modes: does reproductive mode affect dispersal? Evol. Ecol. https://doi.org/10.1007/s10682-018-9957-0.
Martínez-Freiría, F., Sillero, N., Lizana, M., Brito, J.C., 2008. GIS-based niche models identify environmental correlates sustaining a contact zone between three species of European vipers. Divers. Distrib. 14, 452–461.
Martínez-Freiría, F., Velo-Antón, G., Brito, J.C., 2015. Trapped by climate: interglacial refuge and recent population expansion in the endemic Iberian adder *Vipera seoanei*. Divers. Distrib. 21, 331–344.
Martínez-Freiría, F., Crochet, P.A., Fahd, S., Geniez, P., Brito, J.C., Velo-Antón, G., 2017. Integrative phylogeographical and ecological analysis reveals multiple Pleistocene refugia for Mediterranean *Daboia* vipers in north-west Africa. Biol. J. Linn. Soc. 122, 366–384.
Martínez-Solano, I., Jockusch, E.L., Wake, D.B., 2007. Extreme population subdivision throughout a continuous range: phylogeography of *Batrachoseps attenuatus* (Caudata: Plethodontidae) in western North America. Mol. Ecol. 16, 4335–4355.
Merabet, K., Sanchez, E., Dahmana, A., Bogaerts, S., Donaire-Barroso, D., Steinfartz, S., Joger, U., Vences, M., Karar, M., Moali, A., 2016. Phylogeographic relationships and shallow mitochondrial divergence of Algerian populations of *Salamandra algira*. Amphib. Reptil. 37, 1–8.
Merow, C., Smith, M.J., Silander, J.A., 2013. A practical guide to MaxEnt for modeling species' distributions: what it does, and why inputs and settings matter. Ecography 36, 1058–1069.
Nicolas, V., Mataame, A., Crochet, P.A., Genie, P., Ohler, A., 2015. Phylogeographic patterns in North African water frog *Pelophylax saharicus* (Anura: Ranidae). J. Zool. Syst. Evol. Res. 53, 239–248.
Oliver, M.A., Webster, R., 1990. Kriging: a method of interpolation for geographical information systems. Int. J. Geogr. Inf. Sci. 4, 313–332.
Pereira, R., Martínez-Solano, I., Buckley, D., 2016. Hybridization during altitudinal range shifts: nuclear introgression leads to extensive cyto-nuclear discordance in the fire salamander. Mol. Ecol. 25, 1551–1565.
Peakall, R., Smouse, P.E., 2012. GenALEx 6.5: genetic analysis in Excel. Population genetic software for teaching and research-an update. Bioinformatics 28, 2537–2539.
Phillips, S.J., Anderson, R.P., Schapire, R.E., 2006. Maximum entropy modeling of species geographic distributions. Ecol. Model. 190, 231–259.
de Pous, P., Metallinou, M., Donaire-Barroso, D., Carranza, S., Sanuy, D., 2013. Integrating mtDNA analyses and ecological niche modelling to infer the evolutionary history of *Alytes maurus* (Amphibia; Alytidae) from Morocco. Herpetol. J. 23, 153–160.
Pritchard, J.K., Stephens, M., Donnelly, P., 2000. Inference of population structure using multilocus genotype data. Genetics 155, 945–959.
Quezel, P., Barbero, M., 1993. Variations climatiques au Sahara et en Afrique sèche depuis le Pliocene: enseignements de la flore et de la végétation actuelles. Revue d'Ecologie – la Terre et la Vie 24, 191–202.
Recknagel, H., Jacobs, A., Herzyk, P., Elmer, K.R., 2015. Double-digest RAD sequencing using Ion Proton semiconductor platform (ddRADseq-ion) with nonmodel organisms. Mol. Ecol. Resour. 15, 1316–1329.
Rice, W., 1989. Analyzing tables of statistical tests. Evolution 43, 223–225.
Rodríguez, A., Burgon, J.D., Lyra, M., Irisarri, I., Baurain, D., Blaustein, L., Göcmen, B., Künzel, S., Mable, B., Nolte, A.W., Veith, M., Steinfartz, S., Elmer, K.R., Philippe, H., Vences, M., 2017. Inferring the shallow phylogeny of true salamanders (*Salamandra*) by multiple phylogenomic approaches. Mol. Phylogenet. Evol. 115, 16–26.
Rousset, F., 2008. GENEPOP'007: a complete re-implementation of the GENEPOP software for Windows and Linux. Mol. Ecol. Resour. 8, 103–106.
Salvi, D., Bisconti, R., Canestrelli, D., 2016. High phylogeographical complexity within Mediterranean islands: insights from the Corsican fire salamander. J. Biogeogr. 43, 192–203.
Stamatakis, A., 2014. RAxML version 8: a tool for phylogenetic analysis and post-analysis of large phylogenies. Bioinformatics 30, 1312–1313.
Steinfartz, S., Küsters, D., Tautz, D., 2004. Isolation and characterization of polymorphic tetranucleotide microsatellite loci in the fire salamander *Salamandra salamandra* (Amphibia: Caudata). Mol. Ecol. Notes 4, 626–628.
Stewart, J.R., Lister, A.M., Barnes, I., Dalen, L., 2010. Refugia revisited: individualistic responses of species in space and time. Proc. R. Soc. Lond. B Biol. Sci. 277, 661–671.
Stuckas, H., Velo-Antón, G., Fahd, S., Kalboussi, M., Rouag, R., Arculeo, M., Marrone, F., Sacco, F., Vamberger, M., Fritz, U., 2014. Where are you from, stranger? The enigmatic biogeography of North African pond turtles (*Emys orbicularis*). Org. Divers. Evol. 14, 295–306.
Tarroso, P., Velo-Antón, G., Carvalho, B., 2015. PHYLIN: An R package for phylogeographic interpolation. Mol. Ecol. Resour. 15, 349–357.
Van Oosterhout, C., Hutchinson, W.F., Wills, D.P.M., Shipley, P., 2004. MICRO-CHECKER: software for identifying and correcting genotyping errors in microsatellite data. Mol. Ecol. Notes 4, 535–538.
Veith, M., Lipscher, E., Öz, M., Kiefer, A., Baran, I., Polymeni, R.M., Steinfartz, S., 2008. Cracking the nut: geographical adjacency of sister taxa supports vicariance in a

polytomic salamander clade in the absence of node support. Mol. Phylogenet. Evol. 47, 916–931.
Veith, M., Mayer, C., Samraoui, B., Donaire-Barroso, D., Bogaerts, S., 2004. From Europe to Africa and vice versa: evidence for multiple intercontinental dispersal in ribbed salamanders (Genus *Pleurodeles*). J. Biogeogr. 31, 159–171.
Velo-Antón, G., Godinho, R., Harris, D.J., Santos, X., Martínez-Freiría, F., Fahd, S., Larbes, S., Brito, J.C., 2012. Deep evolutionary lineages in a Western Mediterranean snake (*Vipera latastei-monticola* group) and high genetic structuring in Southern Iberian populations. Mol. Phylogenet. Evol. 65, 965–973.
Veríssimo, J., Znari, M., Stuckas, H., Fritz, U., Pereira, P., Teixeira, J., Arculeo, M., Marrone, F., Sacco, F., Naimi, M., Kehlmaier, C., Velo-Antón, G., 2016. Pleistocene diversification in Morocco and recent demographic expansion in the Mediterranean pond turtle *Mauremys leprosa*. Biol. J. Linn. Soc. 119, 943–959.
Warren, D.L., Glor, R.E., Turelli, M., 2008. Environmental niche equivalency versus conservatism: quantitative approaches to niche evolution. Evolution 62, 2868–2883.
Worth, J.R.P., Williamson, G.J., Sakaguchi, S., Nevill, P.G., Jordan, G.J., 2014. Environmental niche modelling fails to predict Last Glacial Maximum refugia: niche shifts, microrefugia or incorrect palaeoclimate estimates? Global Ecol Biogeogr. 23, 1186–1197.